

# **Dynamic behaviour in nonporous hybrid metal-organic materials via mechanochemical and gas-solid reactions**

**Fang Guo,\* Hao-Cheng Wang, Antonino Famulari, Hai-Dong Lu and Javier Martí-Rujas\***

## **Contents**

### **1. Materials and methods**

### **2. Single Crystal X-ray Crystallography**

### **3. Synthesis of ligand L**

### **4. Preparation of the chloride salt of L.**

### **<sup>1</sup>H-NMR of protonated ligand**

### **5. Mechanochemical synthesis of 1.**

**Figure S1.** Mechanochemical synthesis of 1.

### **6. Crystal structure of second sphere adduct 1.**

**Figure S2.** Crystal structure of 1 viewed along the *a*-axis.

**Figure S3.** Crystal structure of 1 viewed along the *c*-axis.

**Figure S4.** Simulated XRPD of 1 from SCXRD data.

### **7. Crystal structure of coordination polymer 1'.**

**Figure S5.** (a) Crystal structure of 1' viewed perpendicular to the extension of the 1D polymer chain. (b) Crystal packing viewed along the *c*-axis.

**Figure S6.** Simulated XRPD of 1' from the SCXRD data described above.

### **8. Reversible chemisorption/release of HCl involving the 1D CP 1'.**

**Figure S7.** Structural transformation involving the reversible chemisorption and release of HCl in **1'** (a) and **1** (b). The delimited area marked with red and black points indicates the first and second coordination spheres. Actual images taken of **1'** (c) and **1** (d) before and after the exposure of HCl to **1'**.

### **9. Mechanochemical LAG synthesis of $1'' \cdot \text{MeCN}$ including MeCN.**

**Figure S8.** Synthesis of  $1'' \cdot \text{MeCN}$  including MeCN via LAG.

### **10. Crystal structure of bridging halide complex $1'' \cdot \text{MeCN}$ including MeCN.**

**Figure S9.** Crystal structure of  $1'' \cdot \text{MeCN}$  viewed along the *b*-axis.

**Figure S10.** Crystal structure of  $1'' \cdot \text{MeCN}$  viewed along the *c*-axis.

**Figure S11.** Simulated XRPD of  $1'' \cdot \text{MeCN}$  from SCXRD data.

### **11. Crystal structure of bridged chloride complex $1''' \cdot \text{DMF}$ including DMF. Data obtained from the crystal structure deposited in the CSD OZIFEK.**

**Figure S12.** Crystal structure of  $1''' \cdot \text{DMF}$  viewed along the *b*-axis.

**Figure S13.** Crystal structure of  $1''' \cdot \text{DMF}$  viewed along the *b*-axis.

**Figure S14.** Simulated XRPD of  $1''' \cdot \text{DMF}$  from SCXRD data.

### **12. Hydrochlorination of the bridged chloride complex $1'' \cdot \text{MeCN}$ including MeCN.**

#### **Synthesis of the bridged complex**

**Figure S15.** Pictures showing the blue solid  $1'' \cdot \text{MeCN}$  (a) exposed to vapours of HCl that gave the yellow second sphere adduct **1** (b).

**Figure S16.** Experimental PXRD from single crystal  $1'' \cdot \text{MeCN}$  (a); Experimental PXRD of  $1'' \cdot \text{MeCN}$  exposure to HCl vapor for 48h (b); Simulated PXRD patterns of crystal **1** (c).

### **13. Mechanochemical LAG synthesis of $1''' \cdot \text{DMF}$ including DMF**

**Figure S17.** (a) Simulated XRPD pattern obtained from a single crystal of  $1''' \cdot \text{DMF}$ . (b) Experimental XRPD patterns of  $1''' \cdot \text{DMF}$  obtained by LAG in the presence of

KOH. The peak at  $2\theta$  *ca.*  $28^\circ$  correspond to KCl; (c) Experimental XRPD from single crystal **1**. Inset: powders of **1** (yellow) and **1**'''·DMF (blue) in the LAG reaction.

## 1. Materials and methods

All chemicals were commercially purchased and used as received.

X-Ray powder diffraction (XRPD) patterns were recorded on a Bruker D8 reflection diffractometer at 40 kV, 100 mA for a Cu-target tube and a graphite monochromator.

<sup>1</sup>H-NMR spectra were recorded on a Mercury-Plus 300 spectrometer (VARIAN, 300MHz) at 25°C with TMS as the internal reference.

The TGA experiments were carried out using a Netzsch TG209 F3 thermogravimetric analysis instrument under 20 mL min<sup>-1</sup> N<sub>2</sub> purge. The samples were analyzed from room temperature to 800 °C at a heating rate of 10 °C min<sup>-1</sup>.

## 2. Single Crystal X-ray Crystallography

Crystals were performed on a Bruker P4 diffractometer with Mo K $\alpha$  radiation ( $\lambda = 0.71073 \text{ \AA}$ ). The structures were determined using direct methods and refined (based on F2 using all independent data) by full-matrix least-square methods (Olex-2). Data were reduced by using the Bruker SAINT software. All non-hydrogen atoms were directly located from different Fourier maps and refined with anisotropic displacement parameters. Hydrogen atoms were placed in calculated positions refined using idealized geometries (riding model) and assigned fixed isotropic displacement parameters.

## 3. Synthesis of ligand L

A mixture of pyridine-2-carbaldehyde (2.9 mL, 30 mmol), cyclohexylamine (3.4 mL, 30 mmol) in methanol (35 mL) was prepared and stirred for one day at room temperature. NaBH<sub>4</sub> (1.7 g, 45 mmol) was then added gradually to the resulting solution over 1h. The resulting mixture was allowed to stir for one day at room temperature. The solvent was evaporated under vacuum, and ice was added to quench excess sodium borohydride followed by the addition of water (15 mL). The reaction mixture was extracted with methylene chloride (3 $\times$ 15 mL) and then the combined methylene chloride layer was washed with water (2 $\times$ 15 mL). The methylene chloride layer was

dried on anhydrous sodium sulfate, filtered and evaporated under vacuum to give 4.6 g (80 %) of product **L** as a yellow oil.

#### 4. Preparation of the chloride salt of **L**.

For the synthesis of the chloride salt of **L** 0.095 g (0.5 mmol) were dissolved in 2 mL ethanol and added 5 drops of concentrated HCL, then 3 ml cold diethyl ether was slowly added leading to white precipitate. The precipitate was washed with mixture of ethanol and diethyl ether giving to the chloride salt of **L**. Mp : 120-123°C.

#### <sup>1</sup>H-NMR of protonated ligand

<sup>1</sup>H-NMR (300MHz,DMSO)δ:1.07-1.28 (3H,m,(cyclohexyl-)); 1.38-1.50(2H,m,(cyclohexyl-));1.58-1.62(1H,m,(cyclohexyl-));1.75-1.79(2H,m,(cyclohexyl-));2.11-2.14(2H,m,(cyclohexyl-));3.03(1H,s,(cyclohexyl-));4.38-4.42(2H,m,(-CH2-));7.58-8.74(4H, m, ,H, Py), 9.63 (1H, S, N-H).

#### 5. Mechanochemical synthesis of **1**.

For the LAG synthesis of **1**: 13.1 mg (0.05 mmol) of the chloride salt of **L** and 8.5 mg (0.05 mmol) of CuCl<sub>2</sub>·2H<sub>2</sub>O with a drop of methanol and concentrated hydrochloric acid were ground in an agate mortar for 3 minutes to obtain a yellow powder.

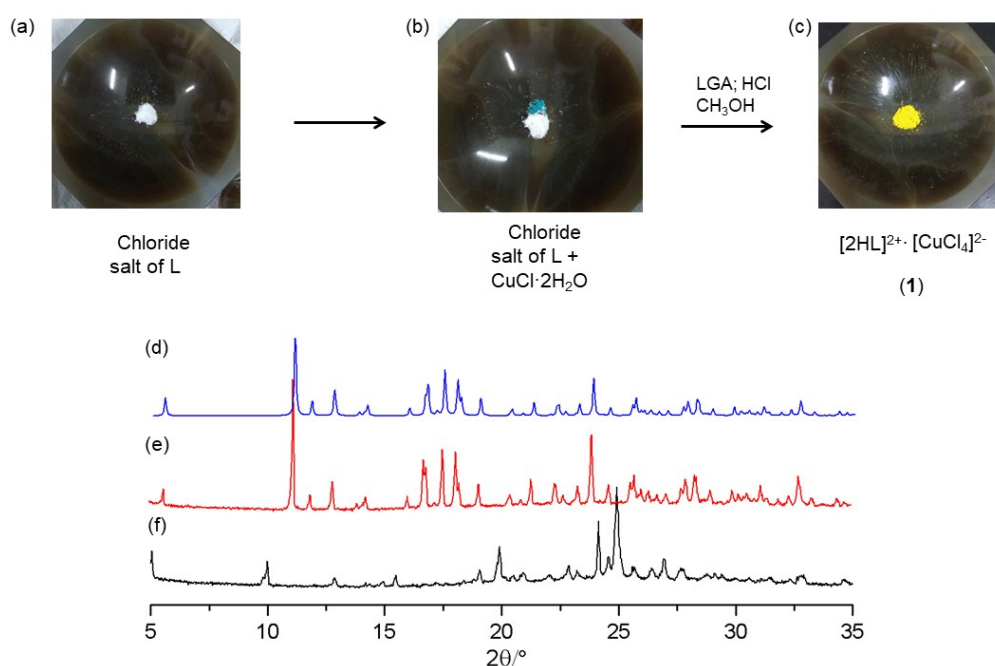


**Figure S1.** Mechanochemical synthesis of **1**.

## 6. Crystal structure of second sphere adduct **1**.

The crystal structure of **1** crystallizes in the monoclinic system in the  $P2_1/c$  (14). The unit cell parameters are:  $a = 6.9225(6)$  Å,  $b = 7.7077(6)$  Å,  $c = 31.930(3)$  Å;  $\alpha = \gamma = 90^\circ$ ;  $\beta = 91.279(2)^\circ$ ;  $V = 1703.25$  Å<sup>3</sup>. **CCDC 1839399**

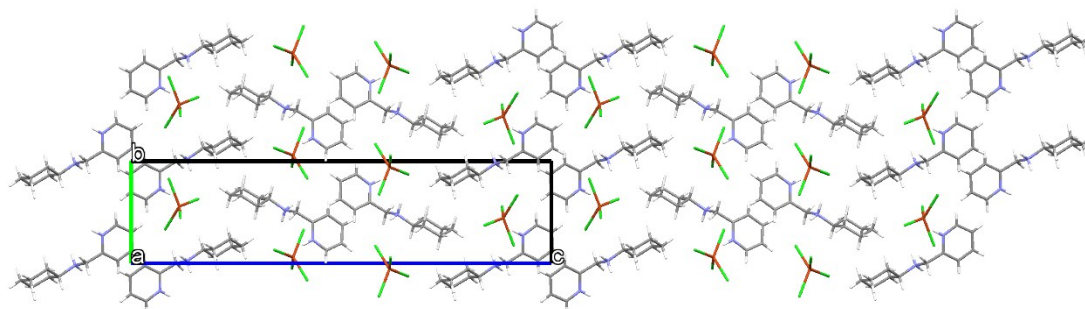


**Figure S2.** Crystal structure of **1** viewed along the  $a$ -axis.

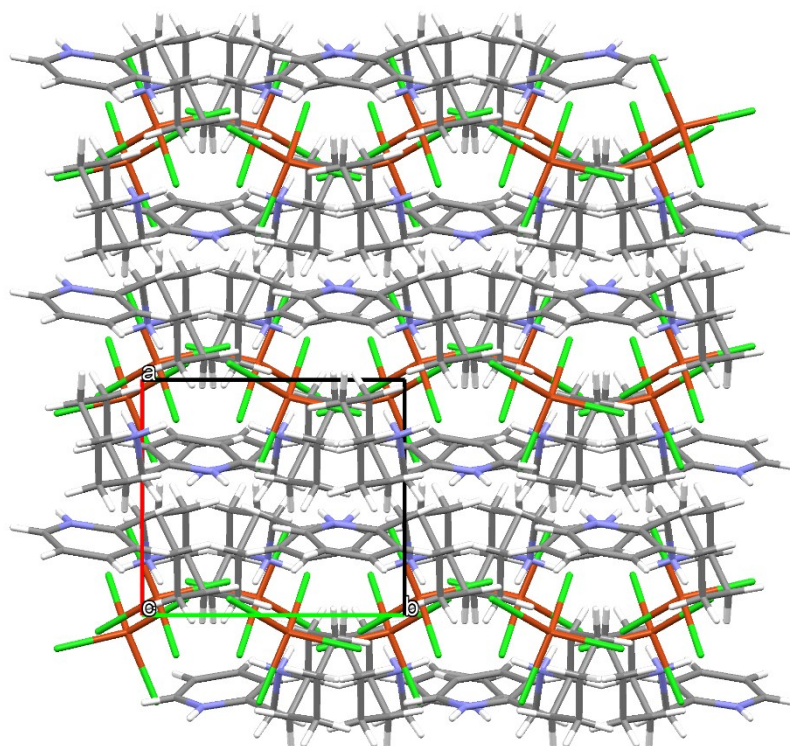


**Figure S3.** Crystal structure of **1** viewed along the  $c$ -axis.

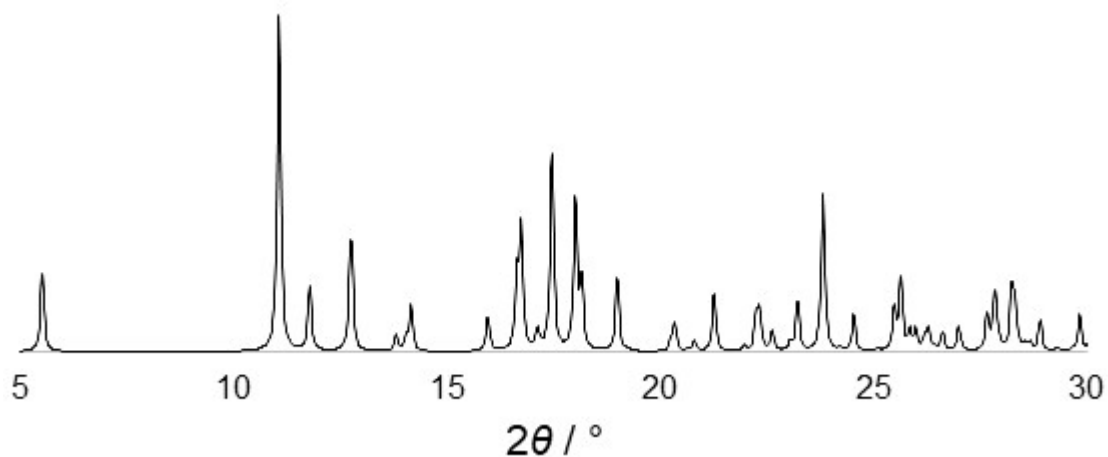


**Figure S4.** Simulated XRPD of **1** from SCXRD data.

## 7. Crystal structure of coordination polymer **1'**.

The crystal structure of **1'** crystallizes in the monoclinic system in the  $Pc$  ( $7$ ). The unit cell parameters are:  $a = 21.2189(18)$  Å,  $b = 8.7496(8)$  Å,  $c = 7.2499(7)$  Å;  $\alpha = \gamma = 90^\circ$ ;  $\beta = 94.387(4)^\circ$ ;  $V = 1342.05$  Å<sup>3</sup>. **Data CCDC 1839405**

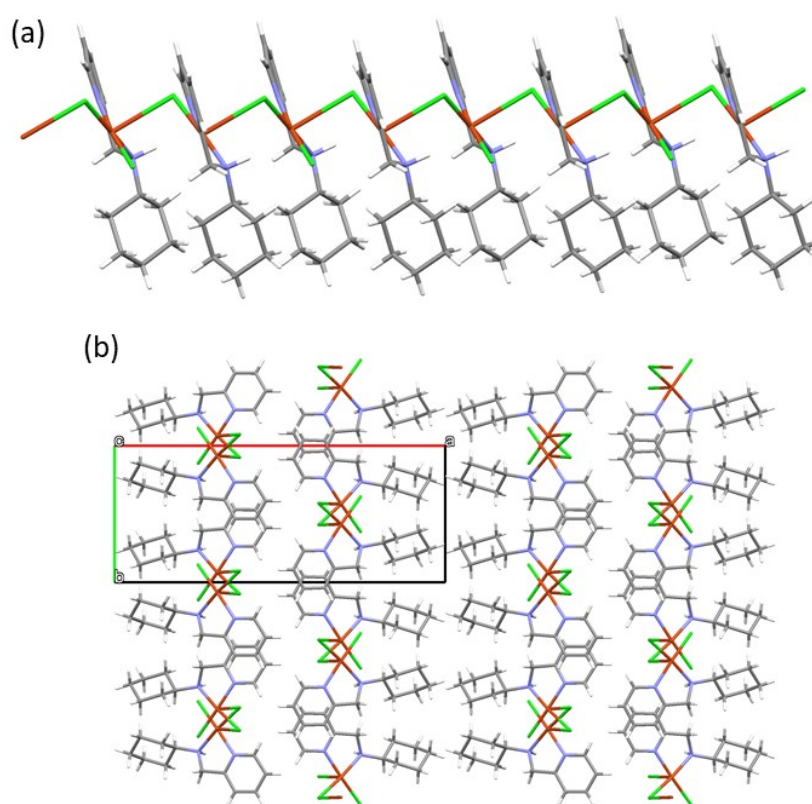


**Figure S5.** (a) Crystal structure of **1'** viewed perpendicular to the extension of the 1D polymer chain. (b) Crystal packing viewed along the  $c$ -axis.

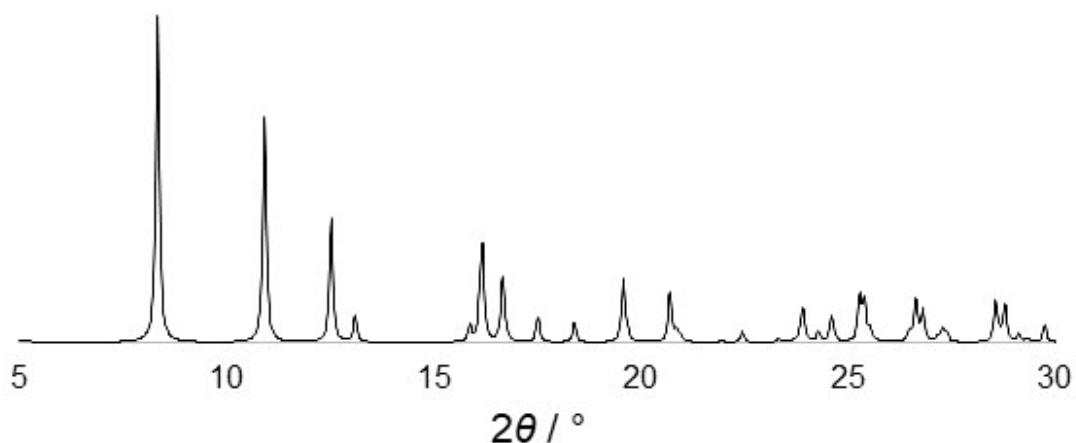


**Figure S6.** Simulated XRPD of **1'** from the SCXRD data described above.

### 8. Reversible chemisorption/release of HCl involving the 1D CP **1'**.

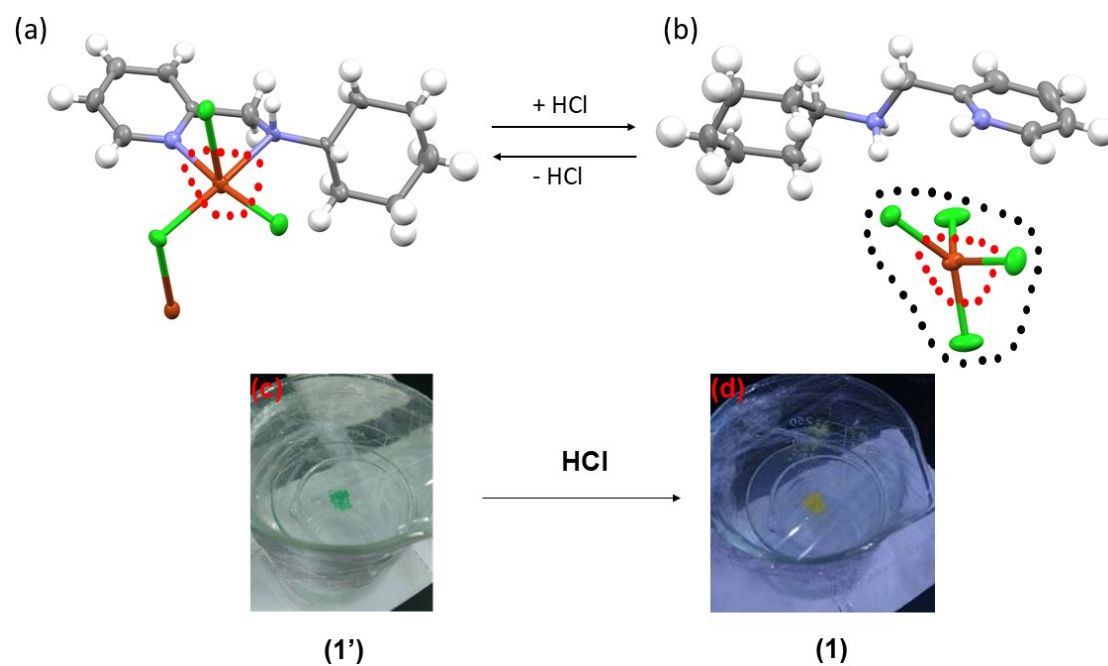


**Figure S7.** Structural transformation involving the reversible chemisorption and release of HCl in **1'** (a) and **1** (b). The delimited area marked with red and black points indicates the first and second coordination spheres. Actual images taken of **1'** (c) and **1** (d) before and after the exposure of HCl to **1'**.

## 9. Mechanochemical LAG synthesis of $1'' \cdot \text{MeCN}$ including MeCN.

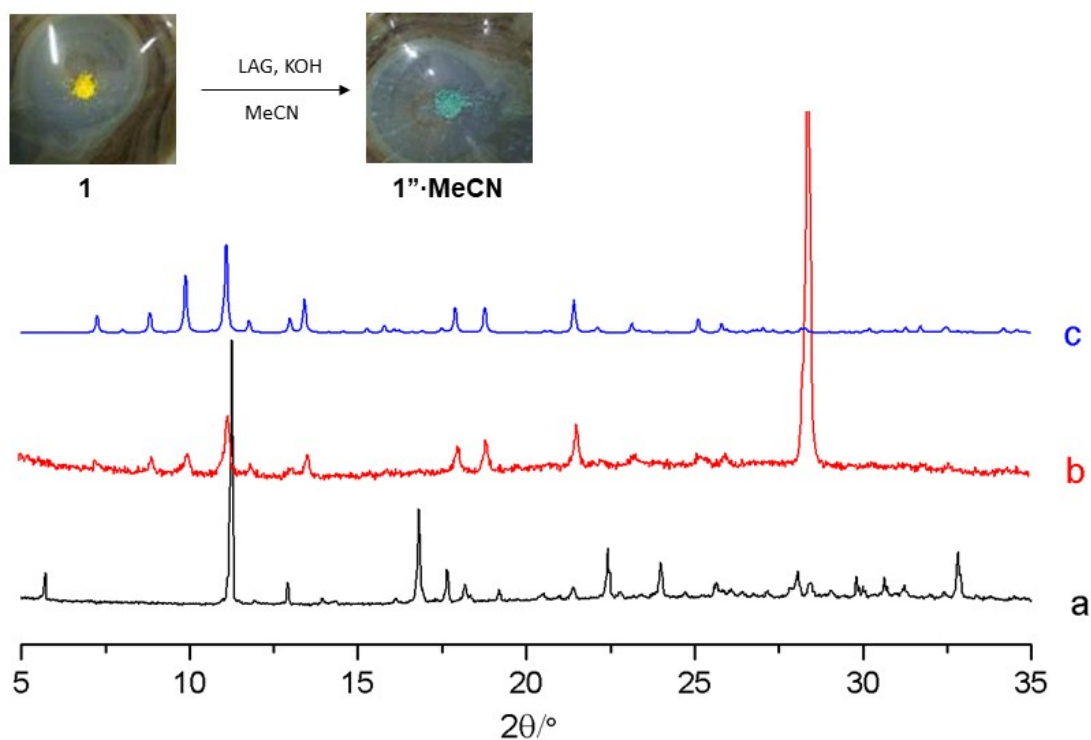


**Figure S8.** Synthesis of  $1'' \cdot \text{MeCN}$  including MeCN via LAG.

## 10. Crystal structure of bridging halide complex $1'' \cdot \text{MeCN}$ including MeCN.

The crystal structure of  $1'' \cdot \text{MeCN}$  crystallizes in the monoclinic system in the  $P2_1/c$  (14). The unit cell parameters are:  $a = 12.1550(8) \text{ \AA}$ ,  $b = 13.1686(9) \text{ \AA}$ ,  $c = 20.0070(13) \text{ \AA}$ ;  $\alpha = \gamma = 90^\circ$ ;  $\beta = 93.363(2)^\circ$ ;  $V = 3196.89 \text{ \AA}^3$ . **CCDC 1839407**

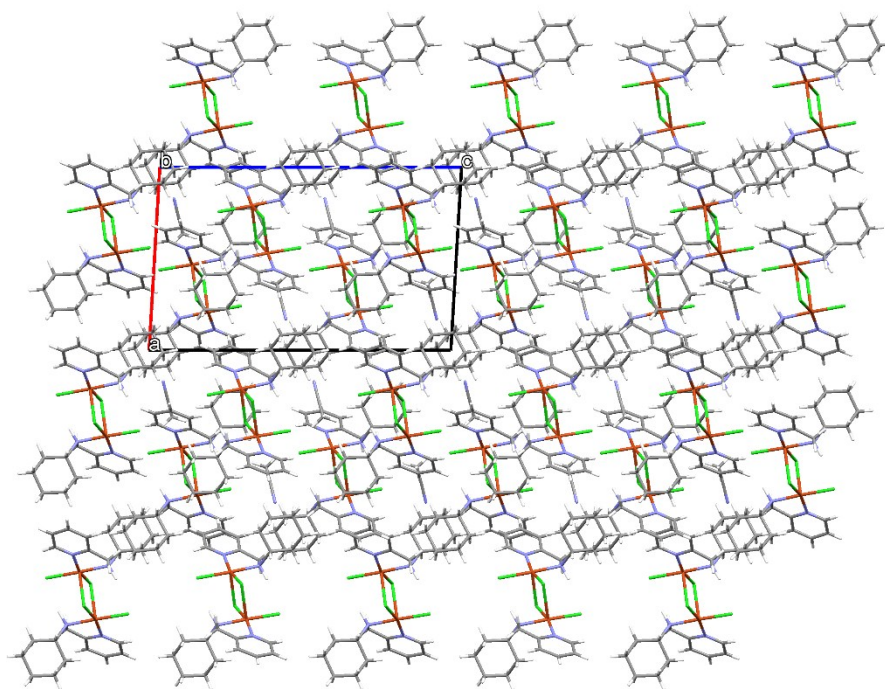


**Figure S9.** Crystal structure of  $1'' \cdot \text{MeCN}$  viewed along the  $b$ -axis.

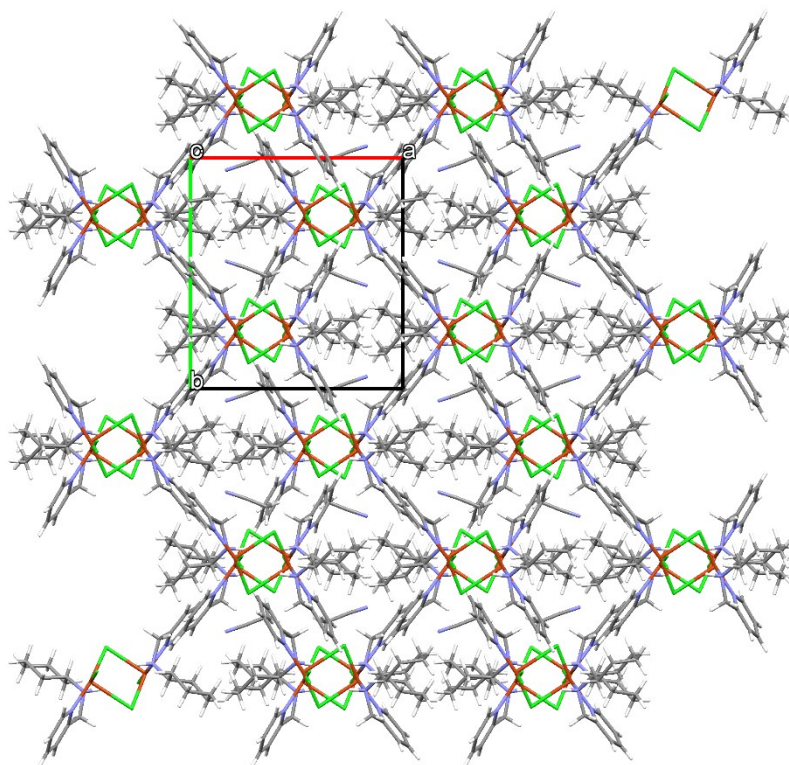


**Figure S10.** Crystal structure of  $1'' \cdot \text{MeCN}$  viewed along the  $c$ -axis.

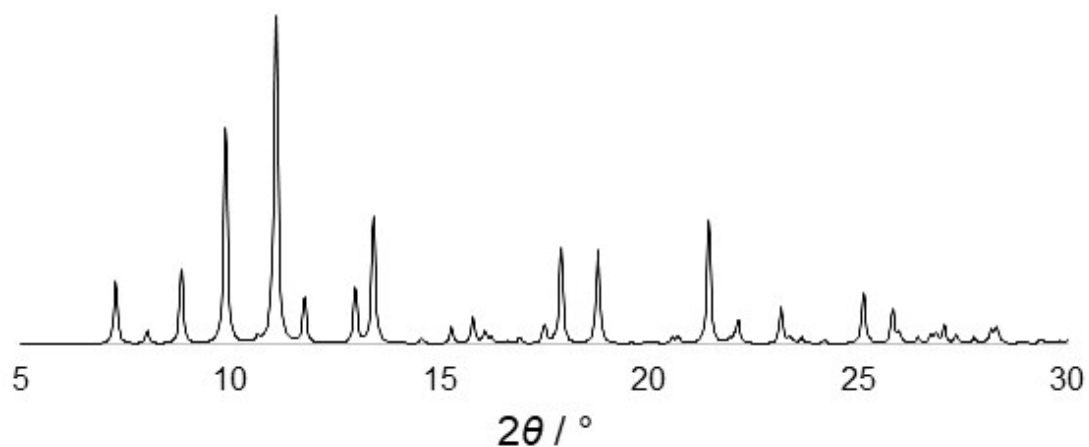


**Figure S11.** Simulated XRPD of  $1''' \cdot \text{MeCN}$  from SCXRD data.

**11. Crystal structure of bridging halide complex  $1''' \cdot \text{DMF}$  including DMF. Data obtained from the crystal structure deposited in the CSD OZIFEK<sup>1</sup>.**

The crystal structure of  $1''' \cdot \text{DMF}$  crystallizes in the monoclinic system in the  $P2_1/c$  (14). The unit cell parameters are:  $a = 12.491(3) \text{ \AA}$ ,  $b = 13.338(3) \text{ \AA}$ ,  $c = 19.756(4) \text{ \AA}$ ;  $\alpha = \gamma = 90^\circ$ ;  $\beta = 92.85(3)^\circ$ ;  $V = 3287.38 \text{ \AA}^3$ .

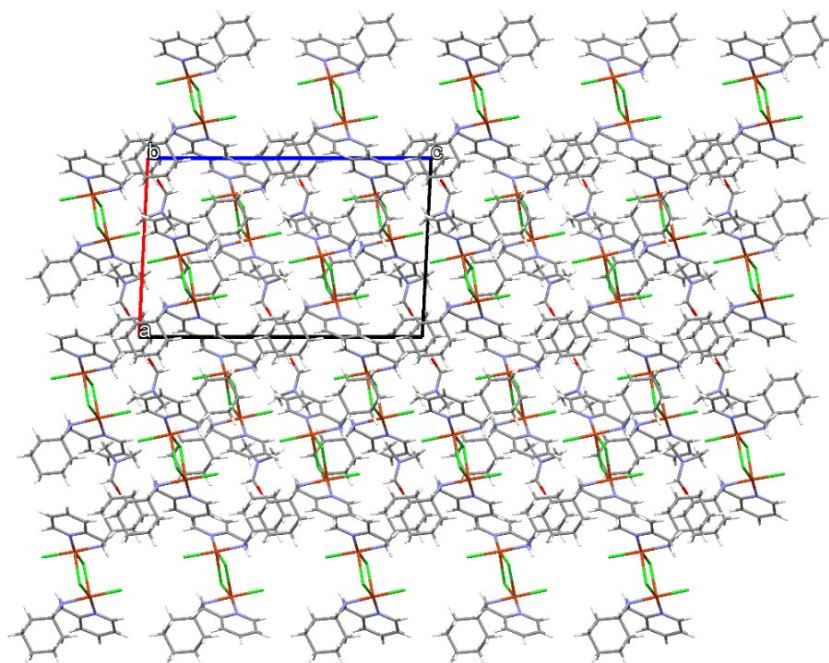


**Figure S12.** Crystal structure of  $1''' \cdot \text{DMF}$  viewed along the  $b$ -axis.

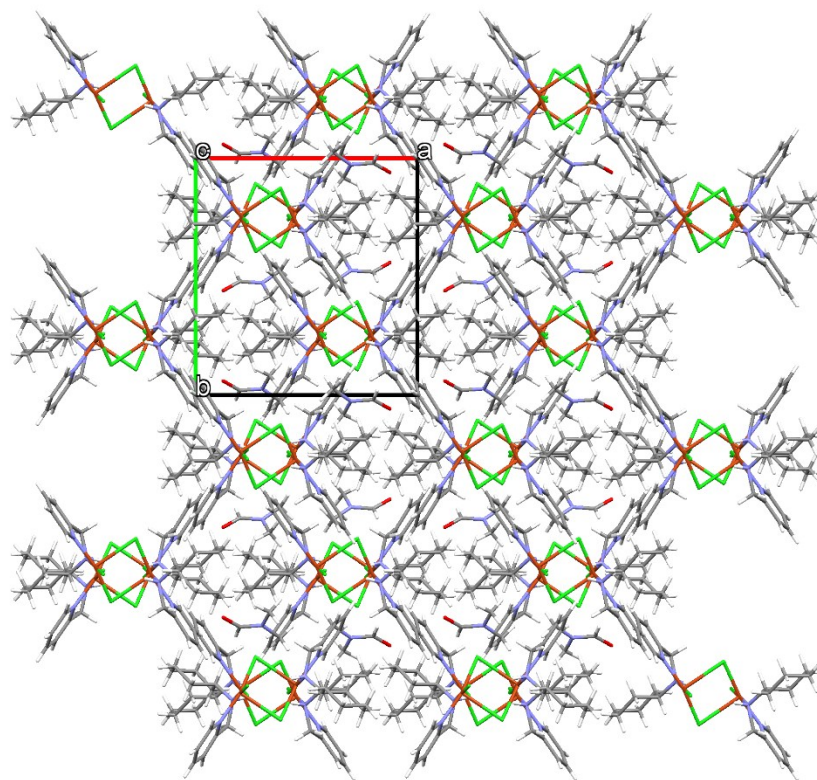


**Figure S13.** Crystal structure of 1'''·DMF viewed along the *b*-axis.

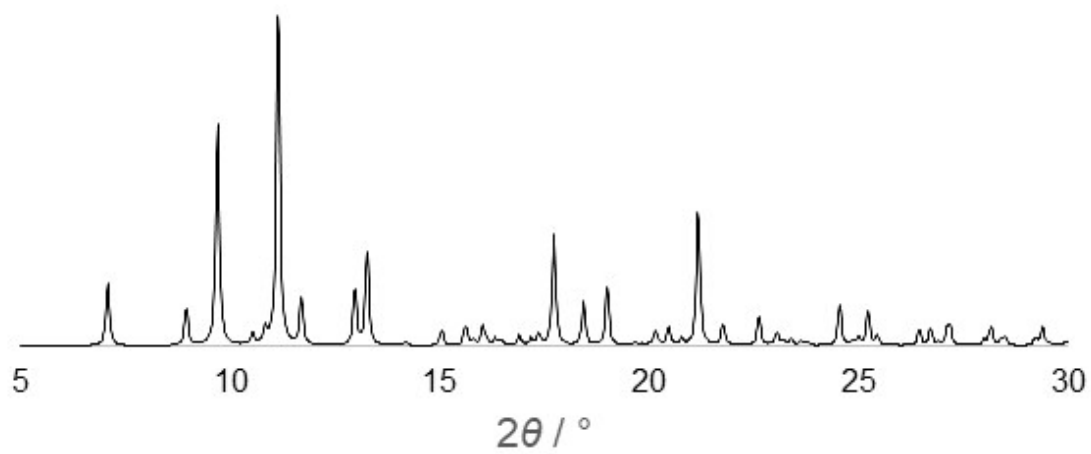


**Figure S14.** Simulated XRPD of 1'''·DMF from SCXRD data.

## 12. Hydrochlorination of the bridged chloride complex $1'' \cdot \text{MeCN}$ including MeCN.

### Synthesis of the bridged complex $1'' \cdot \text{MeCN}$

Preparation of  $1''$ : 19.8 mg (0.05 mmol) of **1** and 5.6mg (0.1 mmol) of **KOH** were ground together for 5 minutes in an agate mortar with two drops of acetonitrile. The resulting blue powder was dried under vacuum for 10 minutes.

Chemisorption reaction: (**1**) The blue powder was placed in a vial inside a sealed jar containing a concentrated HCl solution. The blue powder became yellow in 48 hours.

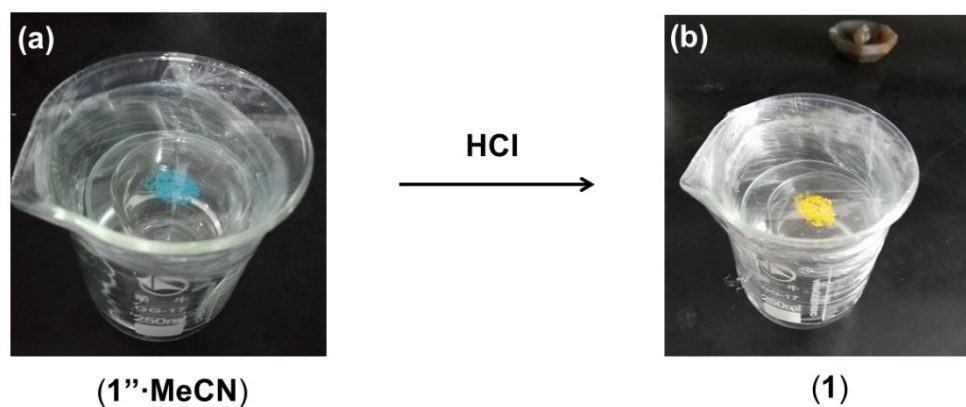


**Figure S15.** Pictures showing the blue solid  $1'' \cdot \text{MeCN}$  (a) exposed to vapours of HCl that gave the yellow second sphere adduct **1** (b).

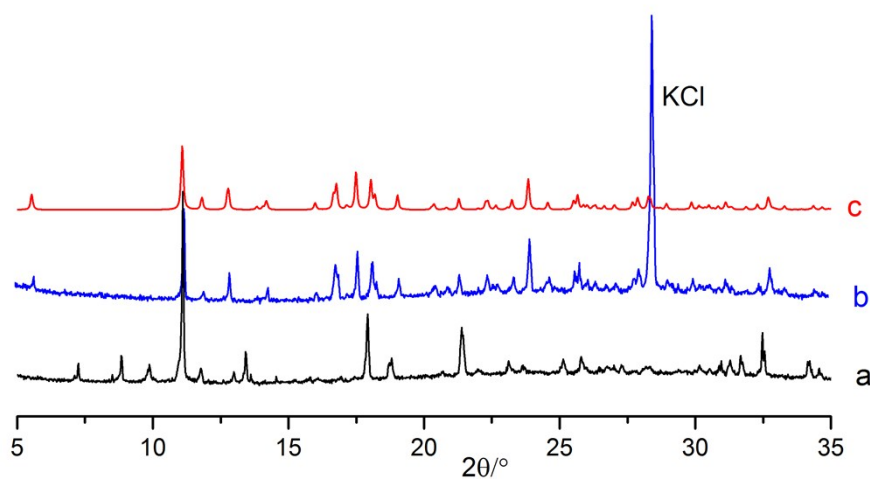


**Figure S16.** Experimental PXRD from single crystal **1''**·MeCN (a); Experimental PXRD of **1''**·MeCN exposure to HCl vapor for 48h (b); Simulated PXRD patterns of crystal **1** (c).

### 13. Mechanochemical LAG synthesis of $1''' \cdot \text{DMF}$ including DMF

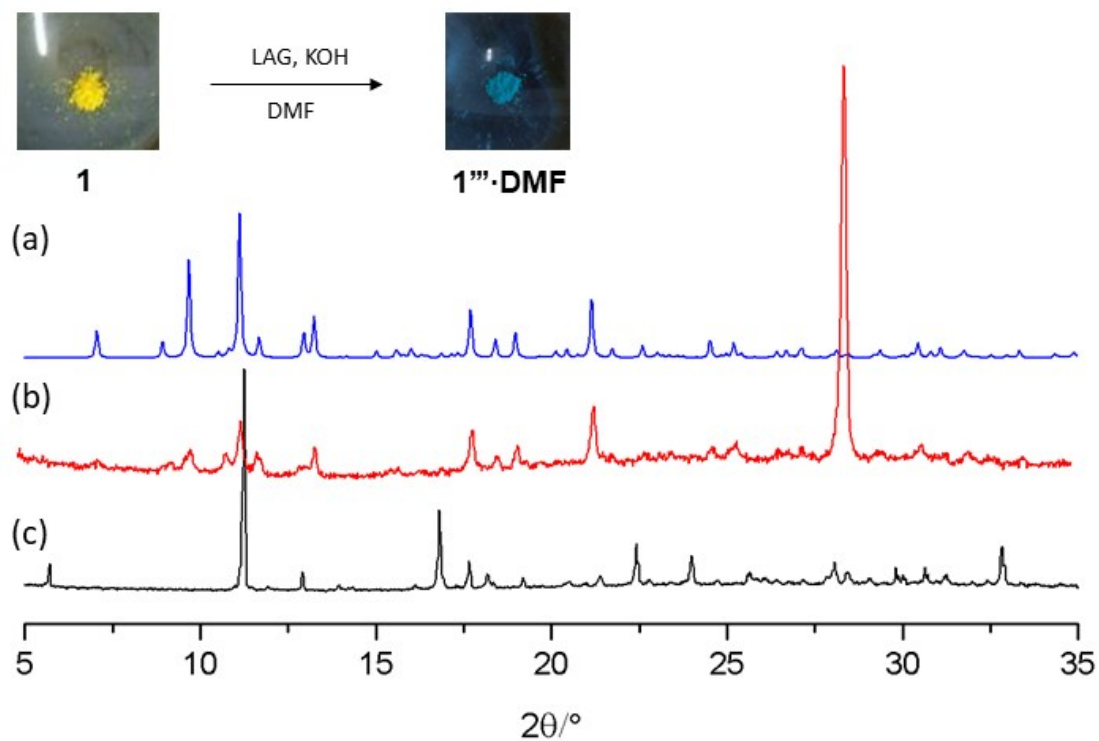


**Figure S17.** (a) Simulated XRPD pattern obtained from a single crystal of  $1''' \cdot \text{DMF}$ . (b) Experimental XRPD patterns of  $1''' \cdot \text{DMF}$  obtained by LAG in the presence of KOH. The peak at  $2\theta$  ca.  $28^\circ$  correspond to KCl; (c) Experimental XRPD from single crystal **1**. Inset: powders of **1** (yellow) and  $1''' \cdot \text{DMF}$  (blue) in the LAG reaction.

### References

1. H. Golchoubian and S. Nateghi, *J. Coord. Chem.*, 2016, **69**, 3192.